Part II: Modelling Erosion and Soil Erosion Risk

9 Model DESER

The conceptual model DESER is designed to **d**etermine **e**rosion and **s**oil **e**rosion **r**isk for semi-arid to semi-humid catchments in developing countries.

The model is a basis for the future development of a decision making tool for regional planners. It is consciously designed to work without large input parameter sets that require multiply resources. This approach makes it useful for non-developed countries where resources to obtain data are often limited. However, the model is scientifically based and in conjunction with the verification of the employed input parameters and their weighting within the model, the modelling quality feasible for estimating the erosion and soil erosion risk is ensured. Figure 87 illustrates the decision tree of the model.

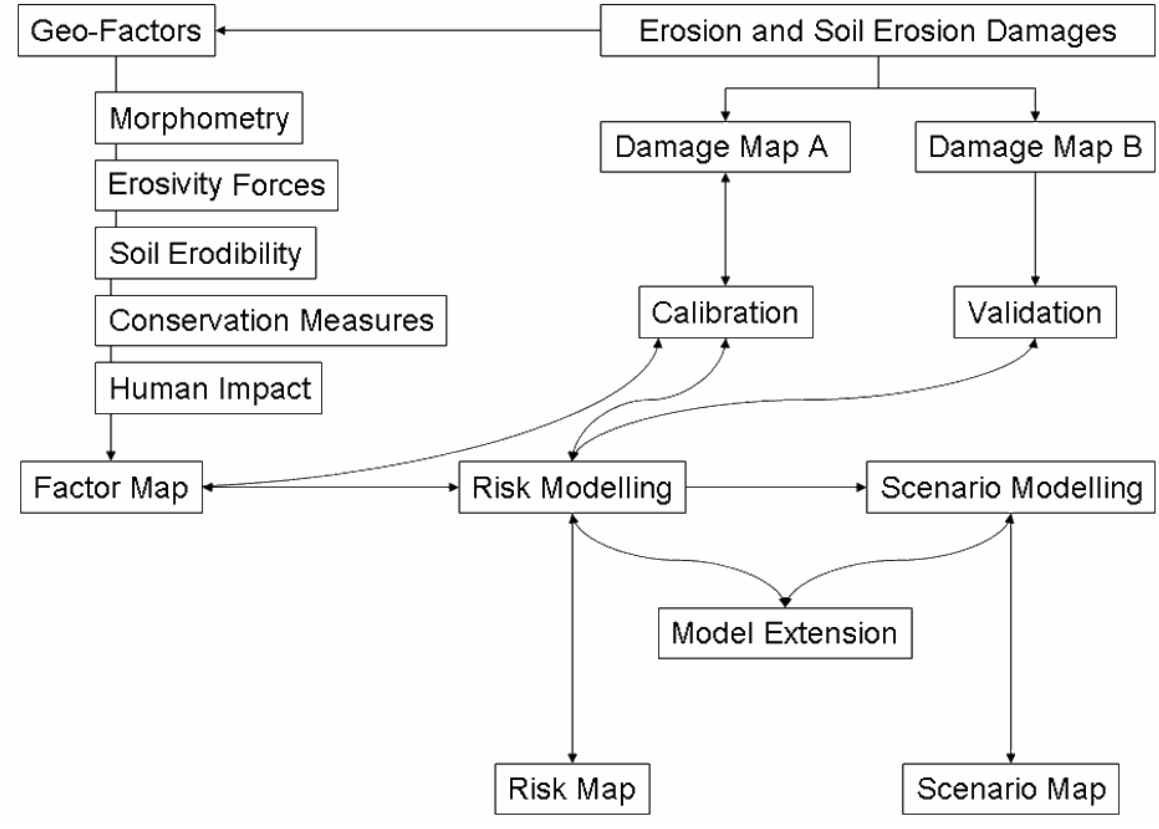

Fig. 87: Decision Tree of the Model DESER

9.1 Modelling Approach

9.1.1 Input Factors

The availability of input data for the computation of the actual erosion and soil erosion risk is limited in most developing countries. For this research, all input parameters, both spatially distributed data and vector or point data, have been converted and adapted to a data grid with a size of 100 by 100 meters. Physically based data are the digital elevation model and its derivations, namely slope, flow accumulation (based on the flow direction) and complex relief curvature (based on the difference of plan relief curvature value minus profile relief curvature value). These data are the basis of the DESER model. Ground data such as soil type, grain size distribution, stone cover and organic carbon content have been added into the model as a correction factor in a second step. Land cover, reflecting land-use and vegetation cover, as well as precipitation totals and intensity support the temporal (i.e. seasonal or annual average) modelling objectives. In addition, a human dynamics factor was added to the model, which reflects the influence of settlements and migration of humans and livestock on physical soil properties.

The overall aim of the model is that it should be very easy to understand and universally applicable in developing countries. Considering these aims, physically based computation principles are rarely used and adapted in this model. The computational principles used in DESER are partially based on the computations of AUERSWALD (1987) as well as WISCHMEIER & SMITH's (1978) empirical universal soil loss equation (USLE). AUERSWALD (1987) analyzed the sensibility of erosion and soil erosion causing factors for the ABAG (‘*allgemeine Bodenabtragsgleichung’*), the German equivalent to USLE. Dominant physical factors influencing the erosion and soil erosion risk are the K-factor, length and inclination of the slopes, as well as complex relief curvature. The erosivity is determined by the amount and intensity of rainfall. Due to insufficient rainfall data both in availability and temporal resolution, the erosivity factor for the DESER model can only estimate trends in actual erosivity.

The development of this model is based on (1) empirical experiences in monitoring processes resulting in erosion, soil erosion and accumulation, and (2) on physical principles that have been used in different erosion and soil erosion models, such as USLE and its variations or the Water Erosion Prediction Project (WEPP). Empirical experiences include research projects carried out in Prince-Edward-Island, Canada (EDWARDS ET AL., 1995, 2000), in South-East Spain (HILL & SCHÜTT, 2000; SCHÜTT & BAUMHAUER, 2000), in the northern

Ethiopian Highlands (SCHÜTT & THIEMANN, 2001; THIEMANN ET AL., 2005), and in the catchments of the rivers *Hare* and *Bilate* in southern Ethiopia (KRAUSE ET AL., 2004; SCHÜTT ET AL., 2002; SCHÜTT & THIEMANN, 2004, 2005; SCHÜTT ET AL., 2005; BECK ET AL., 2004). The catchment area of the *Bilate River* has been selected in this study for a detailed investigation in detecting and monitoring erosion and soil erosion processes.

In a first step individual algorithms were developed for four test sites. All algorithms utilise the same input factors, which are only weight different. In a second step the weights of the input-factors of all algorithms were changed slightly and adapted to each other and thus, the result is one algorithm that is valid for the entire watershed. The utilised input-factors and the algorithm are described as follows.

Altitude

The digital elevation model (DEM) reflects the altitude of the land surface. HURNI (1982) discussed the dependence of the natural vegetation and farming system on the altitude. Thus, the values of the digital elevation model indirectly indicate the natural and human induced vegetation and the potential energy of surface material related to the receiving stream (SCHÜTT & THIEMANN, 2001).

Slope

AHNERT (1988) describes the correlation of the velocity of surface runoff versus the gradient of slope in relationship to the depth of surface runoff. Figure 88 illustrates: the higher the water depth of surface runoff, the higher is the velocity, and increasing slope inclination leads to disproportionally high surface runoff velocity, especially for high volumes of surface runoff. The basis of this assessment is the equation by MANNING (1889).

$$V = \frac{1}{n} R_h^{\frac{2}{3}} \cdot S^{\frac{1}{2}} \qquad (3)$$

Where:

- V - cross-sectional average velocity (m/s)
- n - Manning coefficient of roughness
- R_h - hydraulic radius (m)
- S - slope of pipe/channel (m/m)

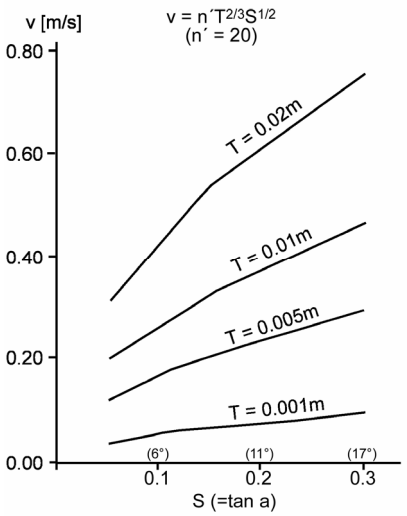

Fig. 88: Velocity of Surface Runoff (Ahnert, 1988)

The effect of slope on erosion and soil erosion has been discussed extensively, for instance by VAN LIEW & SAXTON (1983), GROSH & JARRET (1994) and POESEN (1987).

Flow Accumulation

In the model, increasing slope length, delineated by the flow accumulation, results in increasing erodibility. The correlation between flow accumulation and increasing soil loss is logarithmic: between 0 and 80 m flow accumulation soil loss increases four-fold; flow accumulations larger than 100 m do not result in significant increases in soil loss (AUERSWALD 1987). LAL (1990) analyzes the effect of slope length on runoff, but contrary to AUERSWALD (1987) he predicates that longer slope length lead to more infiltration and therefore to less surface runoff, based on his example for Alfisols in western Nigeria. YAIR & RAZ-YASSIF (2004) describe a negative relationship between frequency and magnitude of runoff and slope length, regardless of the inclination of the slope for the arid to semi-arid Negev Highlands. Continuous surface runoff along a hill slope requires duration of effective rainfall of at least as long as the concentration time, which is always shorter for shorter slope lengths. Depending on the duration of effective rainfall continuous overland flow and sediment removal might decrease with increasing area. Regarding the different soil types, soil properties, as well as duration and amount of effective rainfall in Ethiopia, the factor flow accumulation will be assumed as a multiplication factor for soil loss (MCCOOL ET AL., 1987).

Relief Curvature

The relief curvature is the second derivative of the digital elevation model and describes the flexion of the relief surface. SHARY ET AL. (2002) illustrate the effects of converting and diverting overland flow on erosion and accumulation processes. Profile

concave and plan concave relief elements are causing converting overland flow and thus, increase the energy of surface runoff. In contrast, profile convex and plan convex relief elements are diverting overland flow and here the energy of surface runoff decreases. Increasing surface runoff energy causes erosion, whereas decreasing energy leads to accumulation. Moreover, the gradients and lengths of slopes have to be considered, since they can sometimes cause contrary effects.

Erodibility Correction

The input factor 'erodibility correction' (EC) used in this model is the multiplication of the soil properties grain size distribution, organic carbon content and stone coverage. The influence of these properties on changing the value of the EC varies: whereas a changing content of stone coverage and the grain sizes silt and fine sand effect the EC strongly, the sand, clay and organic carbon contents have less influence. The higher the stone coverage, the lower is the EC and the higher the content of silt and fine sand, the higher is the resulting EC. The EC is closely linked to the K-factor described by AUERSWALD (1987).

Results and discussion of the analysis of the samples from the profiles prevent ongoing utilisation of these data. The results show no clear pattern of soil properties, neither in vertical nor in horizontal sequence. Thus, only the organic carbon content of the top soil samples were utilised as input for computation of the EC. Since the organic carbon content of the top soils varies only very slightly across the watershed, the error from interpolating from point values into spatial data is neglected. Interpolation was done by utilising the ordinary kriging method. In order to get proper spatial soil data for the whole watershed a very high number of profiles need to be analysed and that is contrary the aim of the model. Therefore, the EC is result of a mixture known from FAO ground data and investigated organic carbon content from samples.

Rainfall

The erosivity is determined by the amount and intensity of rainfall. Several definitions have been established within the last decades and are standardized. VAN DIJK ET AL. (2002) give an explanatory overview of rainfall intensity in relation to kinetic energy and LAL (1998) as well as NYSSEN ET AL. (2005) describe the effects of rainfall erosivity in the tropics.

A relationship between monthly rainfall totals and the altitude is not evident for all months. Nevertheless, these algorithms have been used for modelling the spatial average

monthly rainfall totals. The feasibility of theses algorithms has been verified by comparing the results of modelling with real data from meteorological stations.

Monthly precipitation totals and the rainfall intensity index (RII) that has been developed for this model were used in order to illustrate the change of actual erosion and soil erosion risk throughout the year.

Land cover

A land cover class index (LCCI) was developed that uses either satellite data or ground assessed data. The LCCI can be employed as a representation of land cover as well as land use. The land use and land cover classification system developed by ANDERSON ET AL. (1976) has been used as the basis for designing the LCCI. The normalized difference vegetation index (NDVI) data was not used, as the development of this index requires satellite images (such as Landsat TM) and a strong background in remote sensing. Freely available NDVI data (e.g. from NOAA satellites) do not have the spatial resolution that is needed for this model. In contrast, the LCCI can be easily derived from ground mapping, since the input data are only of six classes.

Anthropogenic activities

The human dynamics factor is only used to represent specific activities by humans and livestock and their influence on physical soil properties. These include the reduction of infiltration capacity due to surface compaction or capturing and accumulation of surface runoff on footpaths. The factor considers two input data: footpaths indicating the movement of humans and livestock, and *tukuls* indicating the population density. Both factors give estimation of locally occurring severe erosion and soil erosion damages, as well as of highly endangered areas due to significant changes of the physical and chemical properties of the soil in the vicinity of footpaths and *tukuls*. The factor human dynamics was derived by digitising signatures from footpath and *tukuls* from topographical maps (TK 50, EMA). These vector data were extended in their width by using buffer zones of 30 meters parallel each vector and subsequently transformed into grid data set.

Figure 89 illustrates geo-factors that influence erosion and soil erosion processes as well as the timeframes of these processes. Since the model DESER is handling average monthly to annual erosion processes in a watershed of ~5,500 km² size relevant geo-factors can be determined based on this selection of factors.

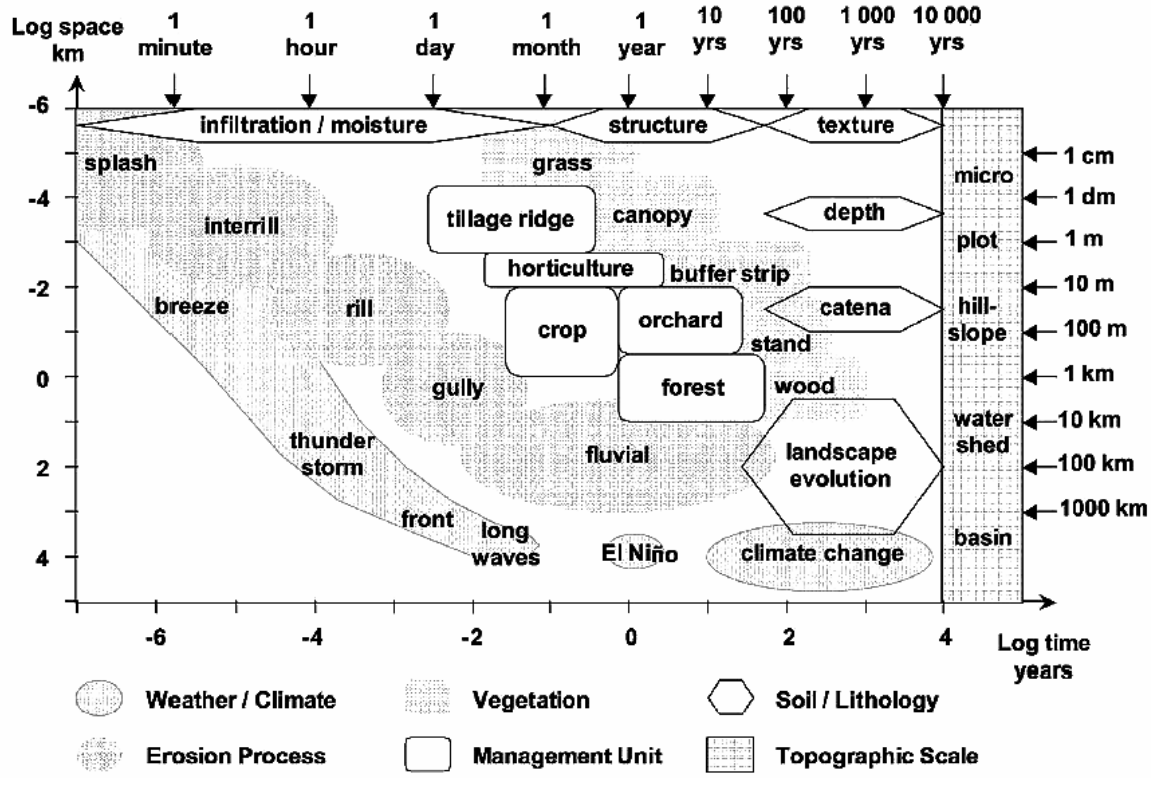

Fig. 89: Geo-factors relevant for Soil Erosion (RENSCHLER & HARBOR, 2002)

9.1.2 Algorithms

The algorithms employed in the model are fairly simple. Preparatory work has to take place in the form of computations of the digital elevation model and the first and second derivatives slope, flow accumulation and complex curvature. Whereas the data of the digital elevation model, slope and complex curvature are used in raw data form, the data from the flow accumulation are reclassified exponentially into 33 classes. The LCCI is consolidated into 6 classes representing different stages of vegetation density from no vegetation (value 1) to very dense green vegetation (value 6).

The EC is calculated by the factors grain size (EC_b), organic carbon content (EC_h) and stone coverage (EC_s) after HENNINGS (1994), whereas the weights of the input data for this equation are changed to contribute the necessity of the developed model.

$$EC = EC_b \bullet EC_h \bullet EC_s \quad (4)$$

$$EC_b = [\text{mean (FAO-texture)}] \bullet 100 \quad (4.1)$$

$$EC_h = 1.15 \bullet C_{org.}\,[\%] \quad (4.2)$$

$$EC_s = (\text{FAO-stonecover}) \bullet 100 \quad (4.3)$$

The FAO data for grain size are provided in values from one to five. These values correlate to the texture classes and factor after HENNINGS (1994) as follows (tab. 22):

Table 22: FAO texture and correlating classes after HENNINGS (1994)

FAO data	texture	factors after HENNINGS (1994)	mean
1	S	0.13	
2	Su2, Su3, Su4, Slu, Sl2, Sl3, Sl4, St2	0.23; 0.35; 0.45; 0.40; 0.20; 0.25; 0.24; 0.11	0.13
3	St3, U, Us, Ul2, Ul3, Ul4, Uls, Ut2, Ut3, Ut4, Lu, Ls2, Ls3, Ls4, Lt2, Lt3, Ltu, Lts, Ts4, Tu3, Tu4	0.10; 0.71; 0.63; 0.66; 0.56; 0.51; 0.50; 0.61; 0.56; 0.48; 0.43; 0.35; 0.27; 0.19; 0.28; 0.21; 0.31; 0.16; 0.09; 0.26; 0.37	0.26
4	Tl, Ts2, Ts3, Ts4,	0.12; 0.04; 0.06; 0.14	0.09
5	T	0.02	0.02

The resulting mean of the factors after Hennings (1994) was utilised in the calculation [mean (FAO-texture)].

The FAO data for stone coverage (FAO-stonecover) are given in percentage. The data are correlating to the factor after HENNINGS (1994) as follows (tab. 23):

Table 23: FAO stone coverage and correlating classes after HENNINGS (1994)

Stone coverage [%]	factor
0 - 1	1
1 - 10	0.87
10 - 30	0.64
30 - 50	0.39
50 - 75	0.19
> 75	0.10

$$EC(mean) = (EC).nrb.mean(50) \quad (5)$$

nrb.mean is a function of ArcView which calculates the mean of 50 neighbourhood grid cell values.

The bases for computing erosion risk are the factors explained above and are represented in the following algorithm.

$$BaseRisk = (DEM /100) - (Class.FlowAccu \bullet Slope^2 \bullet 5) + (CompCurv \bullet 100) \bullet (LCCI) \quad (6)$$

DEM = digital elevation model

Class.FlowAccu = reclassification of flow accumulation

Slope = first derivative from DEM

CompCurv = complex relief curvature

LCCI = land cover class index

The classification of the flow accumulation (Class.FlowAccu; tab. 24) considers the results from research of YAIR & RAZ-YASSIF (2004), AHNERT (1988) and MCCOOL ET AL. (1987).

Table 24: Reclassification of flow accumulation

flow accumulation [number]	class	flow accumulation [number]	class
0 - 5	1	86 - 90	18
6 - 10	2	91 - 95	19
11 - 15	3	96 - 100	20
16 - 20	4	101 - 120	21
21 - 25	5	121 - 150	22
26 - 30	6	151 - 200	23
31 - 35	7	201 - 300	24
36 - 40	8	301 - 450	25
41 - 45	9	451 - 700	26
46 - 50	10	701 - 1000	27
51 - 55	11	1001 - 1500	28
56 - 60	12	1501 - 2500	29
61 - 65	13	2501 - 5000	30
66 - 70	14	5001 - 10000	31
71 - 75	15	10001 - 100000	32
76 - 80	16	100001 - 1000000	33
81 - 85	17		

$$BaseEroRisk = (BaseRisk \bullet EC(mean)).nrb.mean\ (3) \quad (7)$$

nrb.mean is a function of ArcView calculating the mean of 3 neighbourhood grid cell values.

The result BaseEroRisk is classified into 14 classes (tab. 25) representing the potential erosion and soil erosion risk without the influence of precipitation and human activities.

Table 25: Reclassification of the 'BaseEroRisk'

values from computation	class	level of risk
500-1	1	no risk
0- -10	2	
-11 - -20	3	
-21 - -25	4	
-26 - -30	5	
-31 - -50	6	
-51 - -70	7	
-71 - -100	8	
-101 - -150	9	
-151 - -300	10	
-301 - -500	11	
-501 - -700	12	
-701 - -1000	13	
-1001 - -7000	14	severe risk

BaseEroRiskClass = (BaseEroRisk).reclass(14) (8)

The BaseEroRiskClass is modified by the factor erodibility to assess the actual erosion and soil erosion risk:

$$Risk_{(month)} = BaseEroRiskClass \bullet [pre.sum_{(month)} / 100] - [int.index_{(month)} \bullet 20] \quad (9)$$

pre.sum = precipitation total of a individual month

int.index = Rainfall Intensity Index (RII) of the same month

The computation of the amount and intensity of precipitation has been described in chapter 7.1.1.2. Monthly precipitation totals and intensity can be substituted by average yearly values. In a last step, the factor human dynamics is incorporated into the model:

$$Risk.Act = Risk_{(month)} - Hum.dyn \quad (10)$$

Hum.dyn = anthropogenic signs such as footpaths and buildings

In order to accommodate the aim of the model and the qualification of its potential users, only standard software was used for preparing data and for the computation of the model results. Besides Microsoft Office products, the software Erdas Imagine was used for analysing and interpreting the satellite images for the LCCI. Interpolations to compute area wide precipitation was carried out with the software Surfer and Arc View / Arc Info was used for the computation of the model results.

9.2 Results

The map (fig. 90) of the potential erosion and soil erosion risk shows 14 risk classes as a result of the modelling without the localised influence of movement of humans and livestock and without the localised influence of soil conservation measures.

Purple colours represent areas with different degrees of erosion and soil erosion risk, whereas green colours indicate almost no erosion and soil erosion risk; the risk class 1 stands for accumulation areas. The 14 risk classes are heterogeneously distributed throughout the *Bilate* watershed: high values of the risk classes are strongly linked to high values of the slope gradient but also with high values of the flow accumulation. Offsets within the moderate risk classes indicate changes in the erodibility factor or vegetation cover, whereas the classes 1 to 4 are results of smooth slope gradients or flat areas. All classes are influenced by the influence of the complex relief curvature.

In the northern and in the southern centre of the *Rift Valley (2)*, a cluster of low risk classes dominate, except in areas parallel to the stream channels. Another cluster is the hill slope of the relict of a volcano in the northern centre of the *Rift Valley (2)* where moderate risk classes prevail. The third cluster is located in the south-eastern part of the *Rift Valley (2)*. Here, moderate risk classes dominate and only few areas are subject to high to very high erosion risk. In the geomorphological unit *Valleys and Basin (3)* two clusters occur: the basin of the *Bilate Hayk* is a pure accumulation area without any erosion and soil erosion risk. The valleys in the northern part are characterised by moderate risk classes descending to very low risk classes at the bottom of the valleys and in the transition zone to the *Bilate Hayk* basin. Contrary, the *Western Ethiopian Highlands (1)* are dominated by moderate to severe risk classes.

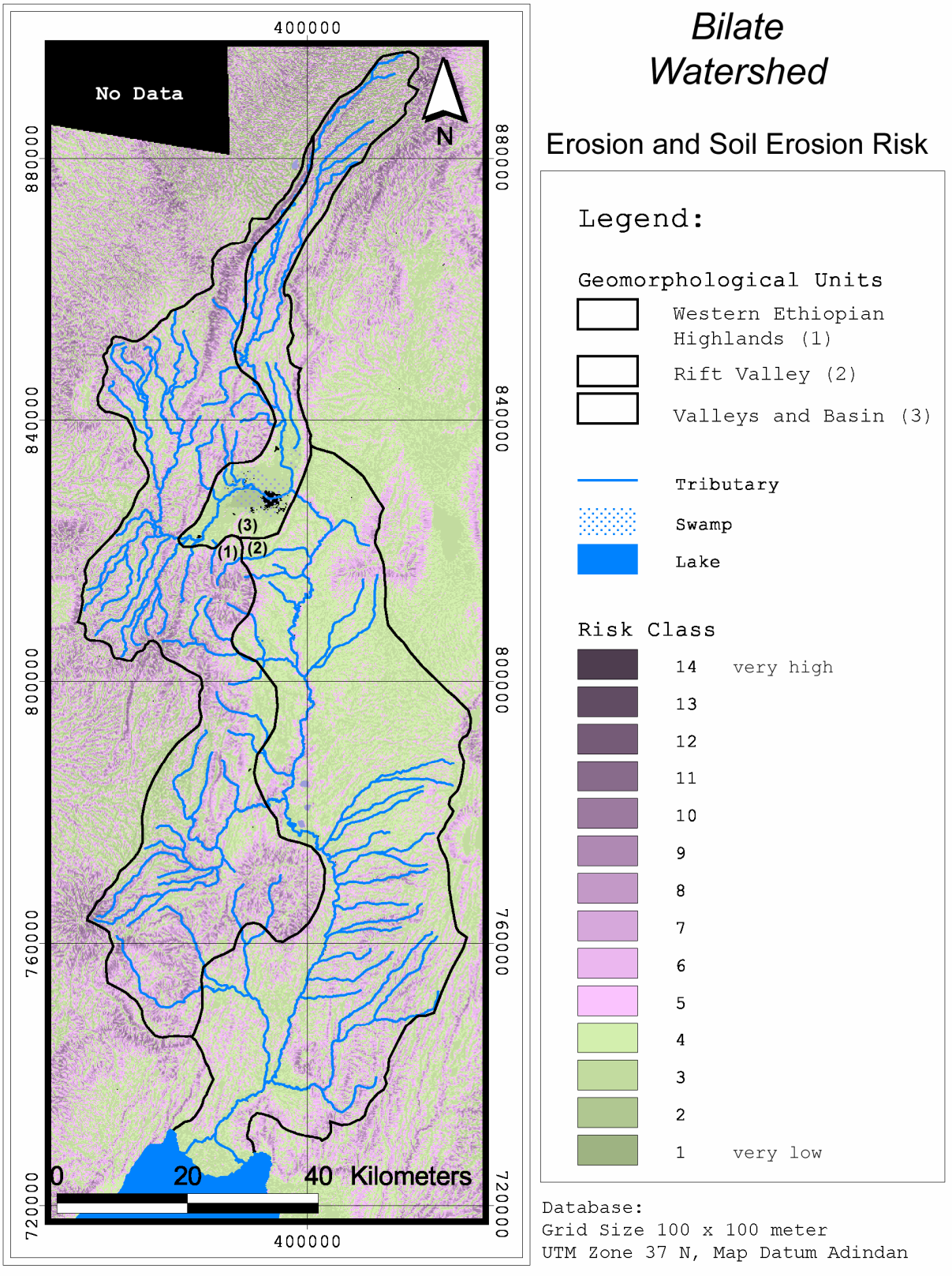

Fig. 90: Erosion and Soil Erosion Risk in the *Bilate* Watershed

The distribution of the risk classes is significantly different for the geomorphological units *Western Ethiopian Highlands* versus *Rift Valley* (significance=0.00, $\alpha<0.05$) but not for *Valleys and Basin* versus *Rift Valley* (significance=0.07; $\alpha<0.05$) and not for *Western Ethiopian Highlands* versus *Valleys and Basin* (significance=0.06; $\alpha<0.05$). The values in table 20 represent the risk class values, which are ranging from 1 (no risk) to 14 (severe risk).

Table 26: Statistics of the Risk Values for the Geomorphological Units

Unit	N	Mean	Std. Dev.
Western Ethiopian Highlands	355	3,29	2,31
Valleys and Basin	95	3,31	2,26
Rift Valley	421	3,89	1,49

The relative distribution of risk classes within the geomorphological units is displayed in figure 91: In all units, the risk classes are distributed bimodally with a major peak for class 2 (low erosion and soil erosion risk) and a minor peak for class 6 (moderate erosion and soil erosion risk). In the *Rift Valley* the highest ratios were computed for low risk classes; more than 80% of the area of the *Rift Valley* is low or very low endangered by erosion and soil erosion risk and only 20% are moderately endangered. The ratios of highly and very highly endangered areas as well as accumulation areas are negligible. In the *Valleys and Basin* the ratio of accumulation area is much higher reaching 14%. But also risk classes of higher values occur intermittently, although they reach not the highest risk class. Moderate risk classes have higher ratiosin the *Valleys and Basin* than in the *Rift Valley*. In contrast, in the *Western Ethiopian Highlands* the ratios of all classes are less pronounced. Low and very low risk classes are reaching less than 30% and the accumulation area has a ratio of 8%. Moderate to high-risk classes have values between 5 and 15%, whereas the very high risk class (14) does not occur.

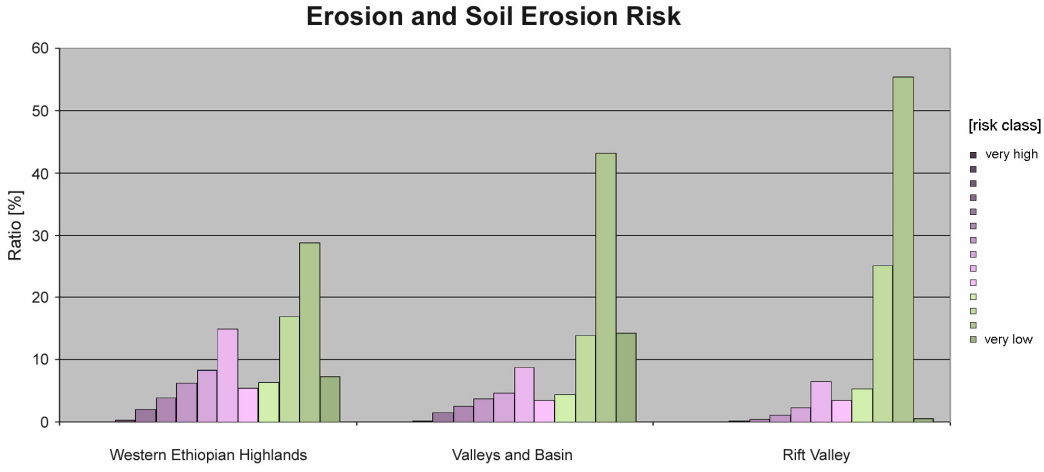

Fig. 91: Distribution of Erosion and Soil Erosion Risk

The detailed map of the potential erosion and soil erosion risk (fig. 92) illustrates the narrow interpretation of the risk from very low (value 1) to high (value 13); value 14 (highest risk class) is not occurring in this modelling exercise. The dominant factors causing these narrow changes are the rapid change of the slope gradients and the sudden changes of the complex relief curvature. These are caused by the very heterogeneous relief character at ground scale and the abrupt transformation from steep relief elements to very gentle slope gradients. In addition, the small-scale pattern of the vegetation cover influences the erosion and soil erosion risk significantly. However, although the grid size of 100 by 100 meters used for modelling allows a very detailed appraisal of the erosion and soil erosion risk, this is not necessarily a true reflection of the actual erosion and soil erosion risk. Uncertainties have to be considered as well as the need for detailed information, since the aim of the model is a regional appraisal of erosion and soil erosion risk. Uncertainties are discussed in further detail below.

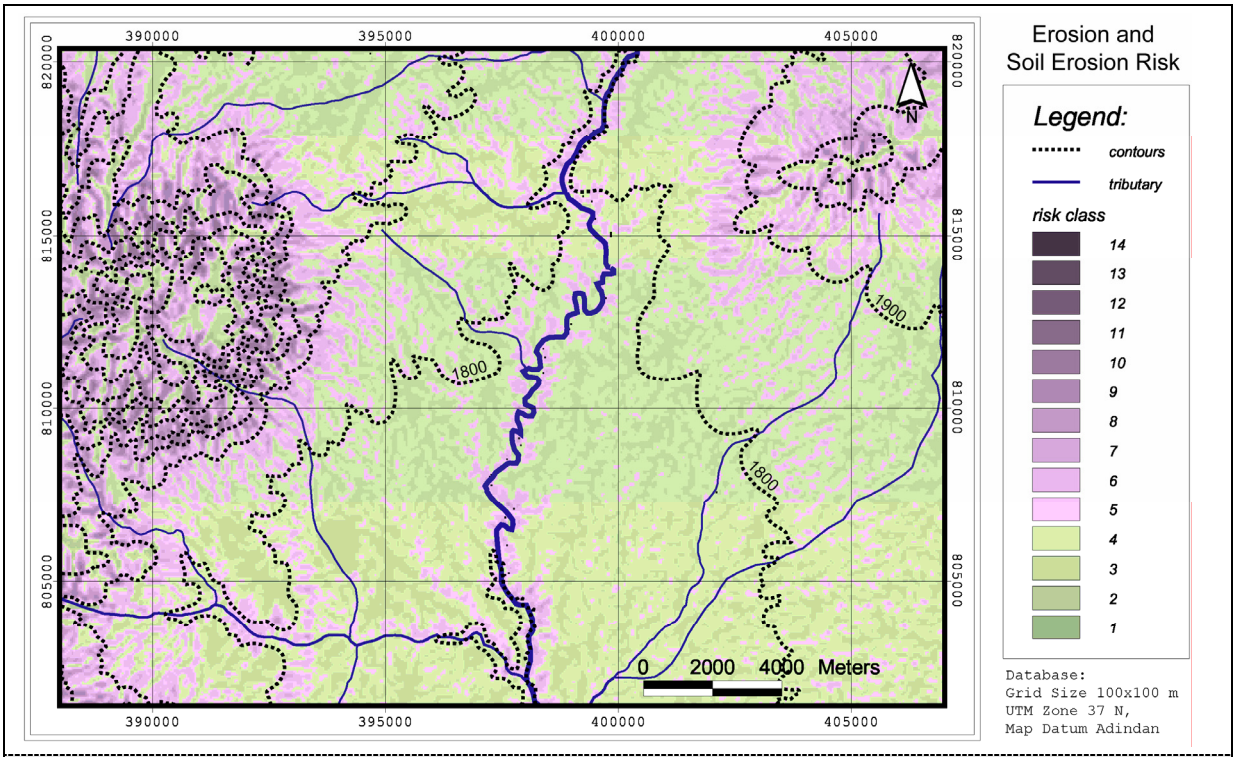

Fig. 92: Potential Erosion and Soil Erosion Risk – Detailed Map of the Central Part of the *Rift Valley* unit

The potential erosion and soil erosion risk is illustrated in figure 92. The actual erosion and soil erosion risk (fig. 93) is enhanced by the rainfall intensity index (RII) and the human activities factor. In this example, which represents the rainy season, the risk classes in certain areas are shifted towards classes of higher risk.

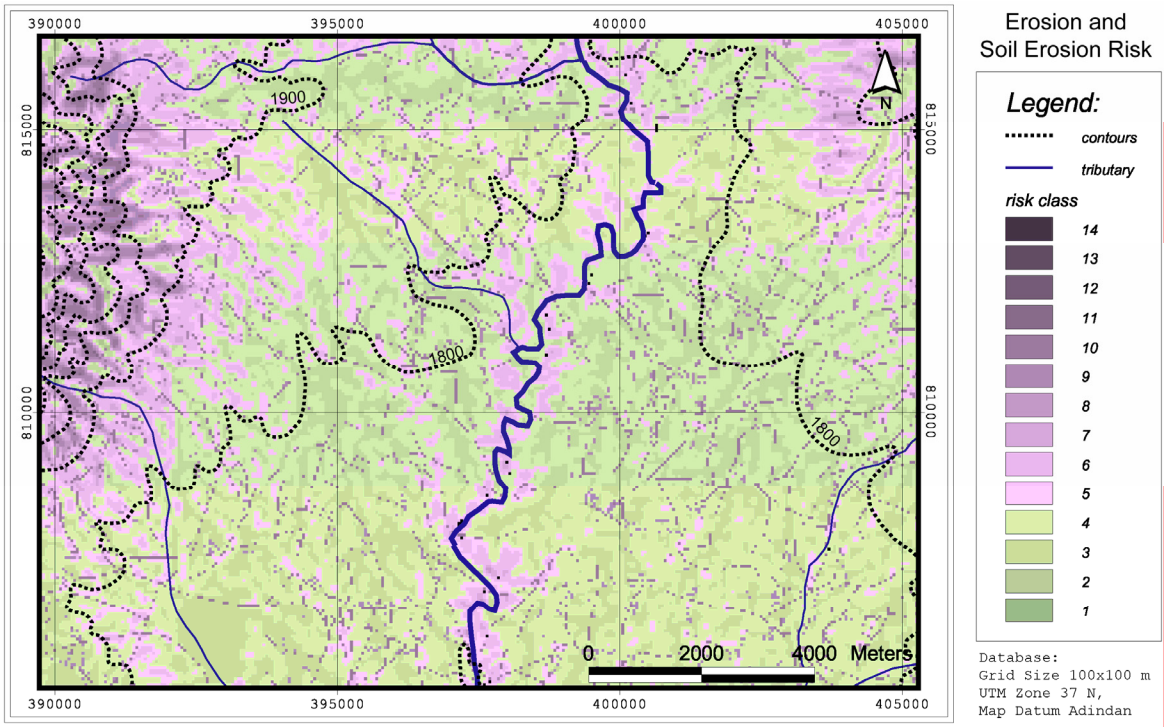

Fig. 93: Actual Erosion and Soil Erosion Risk – Detailed Map of the Central Part of the *Rift Valley*

The influence of movements of humans and livestock on the physical properties of the soil is concentrated in the vicinity of *tukuls* and footpaths. Therefore the transition from areas of very high erosion and soil erosion risk caused by movement to moderate or no erosion and soil erosion risk in the direct vicinity is quite abrupt. Also, these areas are not continuous displayed due to the cell size of the model. The high value of erosion and soil erosion risk near footpaths of 5 m width, which are expanded to 45 m width, cannot always mathematically influence the value of a 100 by 100 m grid, especially when the footpath is located on the borderline of two grid cells.

The generalisation (fig. 95) of the map of the potential erosion and soil erosion risk clearly highlights risk and non-risk areas. A qualitative appraisal of the generalized risk, in contrast to the detailed map of the erosion and soil erosion risk, shows the endangerment of entire regions. In the *Rift Valley* more that 80% of the area are not or only very low at risk (dark green colours); in the *Valleys and Basin* this percentage is more than 50%, and in the *Western Ethiopian Highlands* around 30%. The distribution of the endangered areas is running opposite: the highest ratio of endangered areas is located in the *Western Ethiopian Highlands*, and the lowest ratio in the *Rift Valley*. For the entire catchment of the *Bilate River* the ratio of non endangered areas is significantly higher than for endangered areas, but about 25% of the area is still subject to moderate erosion and soil erosion risk.

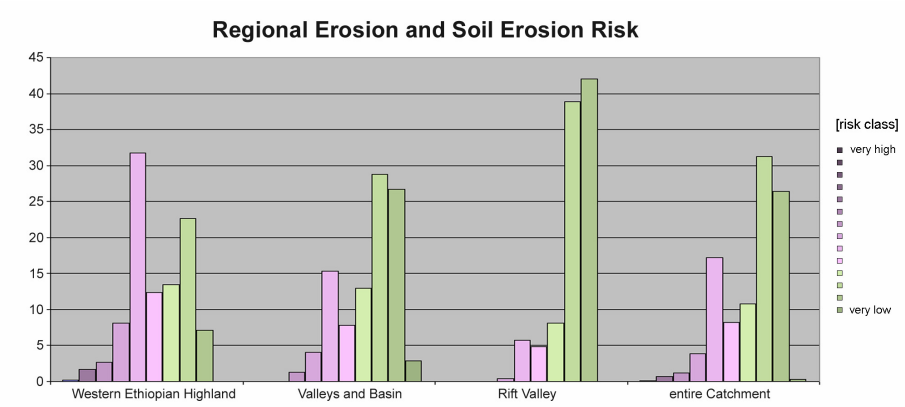

Fig. 94: Distribution of Potential Erosion and Soil Erosion Risk (cells are influenced by neighbourhood five cells)

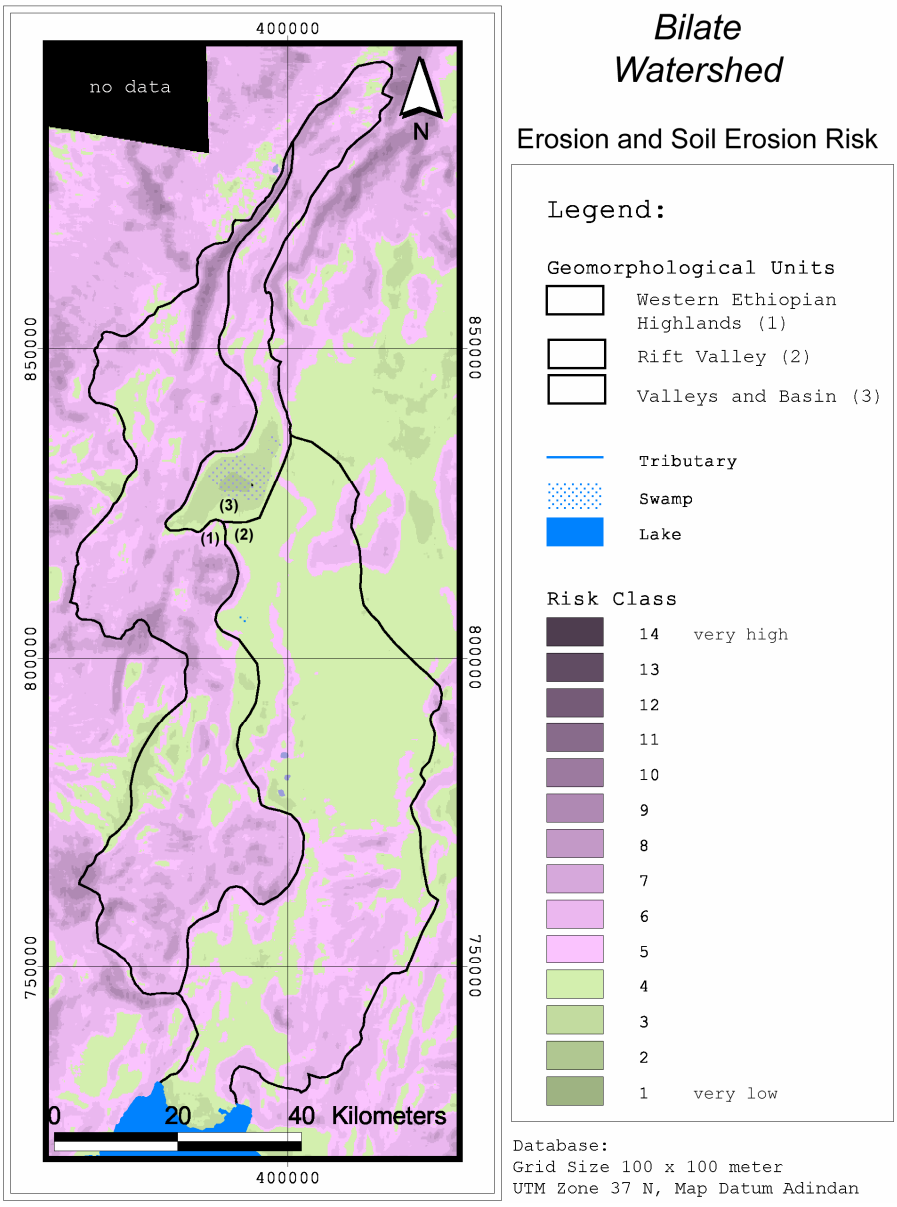

Fig. 95: Potential Erosion and Soil Erosion Risk Classes (Cell values are flattened by values of neighbourhood five cells)

9.3 Discussion

9.3.1 Uncertainty and Sensitivity Analysis

The uncertainty analysis, on one side, focuses on the geo-factors land-cover, precipitation totals and intensity, the DEM and its derivatives, as well as the EC-factor to consider the annual variations. On the other side, the sensitivity analysis was carried out to consider the weighting of the physical input parameters within the model. CROSETTO ET AL. (2000) discuss the uncertainty analysis as uncertainties of the model results caused by uncertainties associated with the input parameters. Sensitivity analysis shows the 'different sources of variations, and how the given model depends upon the information fed into it' (CROSETTO ET AL., 2000). Finally, the uncertainties due to scale effects are discussed.

The input factor land-cover was assigned via remote sensing and satellite images. An unsupervised classification of the channels 1-3 of Landsat TM data in Erdas Imagine resulted in 20 classes, which were manually clustered into 6 classes. Multiple errors are possible: in the tropics satellite images processed during the dry season are often the only ones usable, since cloud cover prevents usable information on ground data during the remainder of the year. As ground data from the dry seasons are used for modelling, natural vegetation or land use throughout the entire year is not reflected. In particular, data of the rainy season are not considered, because the change of active vegetation is not properly known. Here, ground mapping could more accurately determine land use and land cover, which might be feasible in small or medium sized catchments. However, this is not an option for the *Bilate* watershed. In addition, the manual clustering of the unsupervised classification requires very good knowledge of ground data and land use in the research area (JANSEN & DI GREGORIO, 2003). It is a necessity to verify cluster data with end-members collected by partial ground mapping. However, a subsequent correction of clustering the vegetation classes over the entire catchment was not possible; end-members fitting in the southern part of the catchment did not fit well in the northern part. However, uncertainties of the developed land cover classification in the model are considered to be only small, as the model should perform universally in the semi-arid to semi-humid tropics. The classification of only 6 land cover classes allows uncertainties, as each class reflects a wide variety of land cover types. Problems in assessing land use and land cover are discussed by MCCONNELL & MORAN (2001) and FULLER ET AL. (2003). JANSEN & DI GREGORIO (2003) determine land-use and land-cover for the Kiambu district, Kenya and describe assessment as well as decision making rules.

The uncertainty analysis of precipitation totals and intensity is twofold. The raw data, archived from the National Meteorological Services Agency in Ethiopia, show several problems: meteorological stations are not maintained and data collection and storage are strongly constrained by the capacities of the responsible authorities. Next to the typical uncertainties of data collection and storage in Ethiopia, such as improper use of data recording charts, non-standardized calendars, wrong names of meteorological stations or of collected data sometimes result in meaningless data.

Moreover, computing area wide precipitation data based on a limited number of meteorological stations is problematic, particularly in mountainous regions with diverse micro-climates. GOOVAERTS (2000) discusses the geo-statistical approach for incorporating elevation into the spatial interpolation of rainfall. The same technical approach is used in this research. The problems of assessing and quantifying locally occurring storm data were studied by NYSSEN ET AL. (2005) for the northern Ethiopian Highlands.

The erodibility correction factor (EC) is based on the soil properties grain size distribution, stone coverage and organic carbon content. HENNINGS (1994) determines the three individual input parameters for the K-factor utilised partially for USLE and its revised versions. The multiplication of the input parameters results in a K-factor between 0 (no erodibility) and 1 (highest erodibility). BORK (1988) defines the following parameters to determine soil erodibility: grain size distribution, content of organic material, microbial activities, size of aggregates, pore volume, continuity of the pores and soil moisture tension and electric conductivity. In contrast, KÖNIG (1992) suggests using infiltration capacity, grain size distribution, aggregate size, organic material, soil moisture, pH-value, $CaCO_3$, iron and aluminium oxide, clay mineral type and changeable cations as parameters. Both methods require costly and time intensive laboratory analysis, but also give relatively good erodibility values. This might be feasible for case studies in small watersheds or for study plots, but the investigation of all these parameters for the research watershed is not feasible. However, it is known that the determination and utilisation of the EC uses only some factors, but these factors seem to influence the variability of the erodibility quite strongly. VEIHE (2002) concludes for tropical soils in Ghana that the spatial changes in erodibility are mainly caused by changes in the composition of the sand fraction. BRYAN ET AL. (1989) suggest that soil erodibility cannot be defined exclusively, but that a relative ranking of erodibility is needed for each individual study. Dominant factors have to be determined individually for the research areas but also for the specific questionnaire of the investigation. For instance, the

determination of short-term erodibility requires other input parameters than the determination of long-term erodibility (BRYAN ET AL., 1989). Also, WANG ET AL. (2001) discover that soil erodibility changes dynamically and that the determination of the erodibility is more a stable than a variable characteristic and thus, only valid for short-term modelling. DUIKER ET AL. (2001) investigate erodibilities of different soils in south-west Spain and compare their results with erodibility equations used in the 'Water Erosion Prediction Project' (WEPP) Model. Their observed values differ extremely from the computed values of the WEPP model. New approaches to determine soil erodibility are desirable (DUIKER ET AL., 2001).

Considering these uncertainties and the very limited spatial data availability in the watershed, an approach that is based on a small number of parameters with well-known effects (fig. 96) on soil erodibility is more feasible for the DESER model.

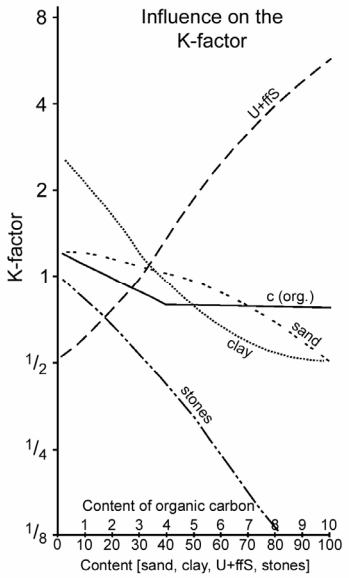

Fig. 96: Variability of the K-Factor due to Content of Organic Carbon and Grain Size Distribution (source: AUERSWALD, 1987)

The data of the erodibility factor were based on data from the FAO and data from laboratory analysis. Several uncertainties also have to be discussed for this data. All samples were taken in the field, whereas the sample locations were selected randomly. It should be noted that most profiles from where the samples were taken are directly associated with the occurrence of gullies, badlands or the rims of barren degraded lands. Thus, the samples are taken from locations, which represent areas of erosion and soil erosion damages. In consequence, the analysis of the samples represent soil and soil erosion properties of vulnerable soils and soil sediments or special relief properties. It is not known whether this analysis is representative for the entire region. However, since only the factors 'organic

carbon content' and 'grain size distribution' (sand fraction) are incorporated into the model, this discussion is obsolete for the uncertainty assessment of the model itself. The uncertainties of laboratory analysis are known for the individual methods, but will not be discussed in detail, since the methods are standardized and probable errors are known for each apparatus.

GIS applications experience a high amount of probable errors, which are rarely discussed in the literature. CROSETTO ET AL. (2000) discuss the uncertainty and sensitivity analyses of spatial models. In general, input values are often of different precision (CROSETTO ET AL., 2000), and thus, an uncertainty analysis requires information of properties of the individual input factors.

Probable errors that were considered in this study are:

a) scale effects

b) geo-referencing of maps and satellite images

c) transformation of vector data into grid data

d) harmonizing grid data

e) interpolation methods

In this research investigations were performed at different scales. Satellite images, FAO data and geological data were of the smallest scale 1:1,000,000; topographic and thematic maps, as well as aerial photographs were of scales between 1:250,000 and roughly 1:40,000; whereas ground mapping was carried out at scale of 1:12,500. Additional scale effects for the interpretation of geomorphological processes were considered, as were time scales, for modelling purchases. RENSCHLER & HARBOR (2002) discuss the importance of considering scale effects for soil erosion assessments and their effects of shifting from local to regional scales. In order to prevent scaling problems, all available spatial data (e.g. such as the digital elevation model and satellite images) were transformed into grid data of 100 by 100 meters cell sizes independently of the utilisation of the data set. Precipitation and ground data were also adapted to this scale. It is known that loss of information occurs when converting from one scale to another and therefore conversions were always before data analyses to minimize these effects. Investigations carried out for the smaller study sites are thus at the same grid size level as the entire watershed. Therefore, information losses occur due to the different scales used for displaying information, but maximal zooming shows the same level of precision of information. Damages were mapped at scale 1:12,500, but since these damages were not incorporated into the model but instead superimposed for calibration and validation,

the different scales are not relevant at maximal zoom level. Only the transformation of digitised signatures from topographical maps (vector data) into grid data resulted in loss of information. The vector data were of maximal extents of 50 meters, whereas the grid data were of 100 meters extent. Thus, the transformation led either to loss of information of the vector data (for example if vector data are located at the border of two or more grid cells) or to a horizontal extension to 100 meters.

Geo-referencing and re-geo-referencing of spatial data sets always result in the shift of the individual grid positions within the dataset. The accuracy of geo-referencing is strongly linked to the original scale. The smaller the scale, the more inaccurate is the geo-referencing, and thus, the superimposition of the different scaled topographical maps, as well as satellite images and aerial photographs lead to uncertainties. Geo-referencing was carried out so that a maximum shift of one grid cell was accepted for all datasets except for the topographical maps. Here, the exactly mapped coordinate systems allowed a more precise geo-referencing.

The interpolation of rainfall data was carried out utilising the ordinary kriging method. This method results in a vector data set that was converted into grid data and thus, the distinct boundaries of the different values (from kriging) shifted due to the location of the grid cells in proximity to the boundary. The linear structures changed into step structures. The uncertainty of utilising the kriging method itself is discussed in chapter 7.1.

A general uncertainty and sensitivity suggestion of this model is the small amount of input parameters. The smaller the numbers of input parameters, the more sensitive the utilised parameters are. Thus, the weightings of the input parameters within the model were considered very carefully. In this model, the weightings are, on one side, based on physically proven methods, and, on the other side, on empirical observations. It is known that important input data such as the actual evapotranspiration or physical soil properties such as the shear strength are missing in this model. They were either not available, or its assessment was too time consuming under consideration of the watershed's size. Attempts to incorporate more than the utilised data did not result in better model results, but in the design of more complex formulas. This was not desirable within the context of the aims of this model. However, prevention of these procedures was one of the main focal points of the development of this model. JETTEN ET AL. (2003) suggest that 'the difficulties associated with calibrating and validating spatially distributed soil erosion models are, to a large extent, due to the large spatial and temporal variability of soil erosion phenomena and the uncertainty associated with

the input parameter values used in models to predict these processes. They will, therefore, not be solved by constructing even more complete, and therefore more complex, models'.

The verification of the actual erosion and soil erosion risk data including human impacts was done by comparing the estimated risk potential to data from a map that shows the amount of soil loss calculated with the USLE (provided from EMA). The USLE map is at scale 1:200,000 and soil loss is classified into eight classes (1=no loss; 8=severe loss), whereas the classes show distinct values of soil loss. The values are ignored, since DESER model is qualitatively.

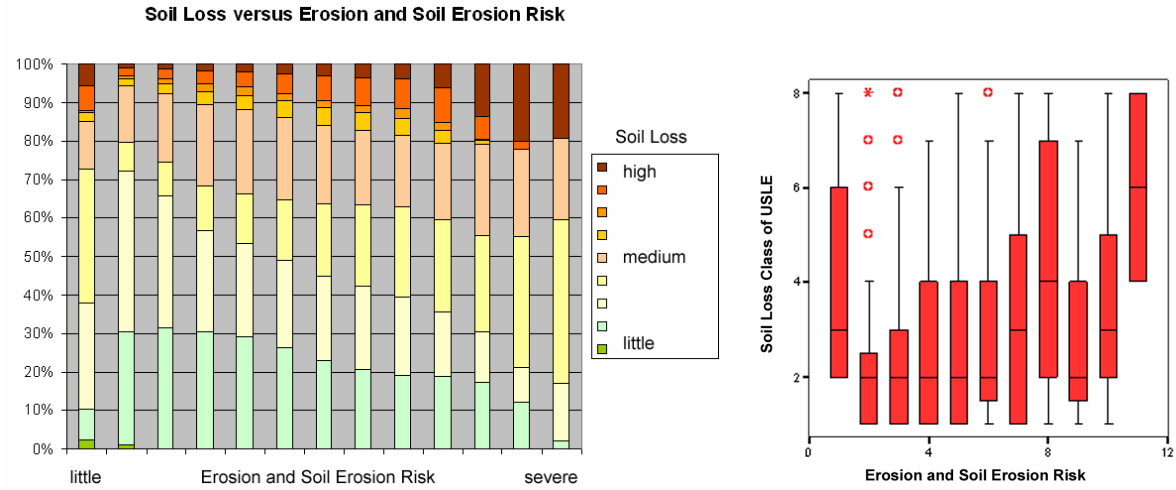

Fig. 97: Soil Loss versus Erosion and Soil Erosion

The data from both models are comparable, as both erosion and soil erosion risk and soil loss were computed for an annual time frame. The correlation of the 8 different soil loss classes versus the 14 erosion and soil erosion risk classes is significant after Pearson ($\alpha<0.01$, n=1,048), whereas one class is outstanding (fig. 97). In this research, the model assumes higher erosion and soil erosion risk classes than predicted soil losses. This is due to the unusual risk of that specific area from the uncommon sequence of the soil (see Chapter 7.2.5).

Also, the superimposition of risk maps on the damage maps show good consistency. Figure 98 displays exemplarily for the study site *Ana* mapped erosion and soil erosion damages, which overly onto the erosion and soil erosion risk map. Areas of moderate to severe erosion and soil erosion risk coincide with areas of damages such as gullies and rills in the centre part of the watershed. Erosion and soil erosion risk increases where the tributary reaches steep slopes. However, in the southern part severe erosion and soil erosion risk is modelled but no damages were recorded. In fact, this area is under recovery: trees were

planted, terraces were constructed and the area is closed for any land use. This indicates a formerly highly damaged and degraded area, but soil conservation measures exist and thus, prevent conclusions about the former condition of this area. However, photographs from distinct areas outside to this watershed also verify both the occurrence and the degree of endangerment to erosion and soil erosion.

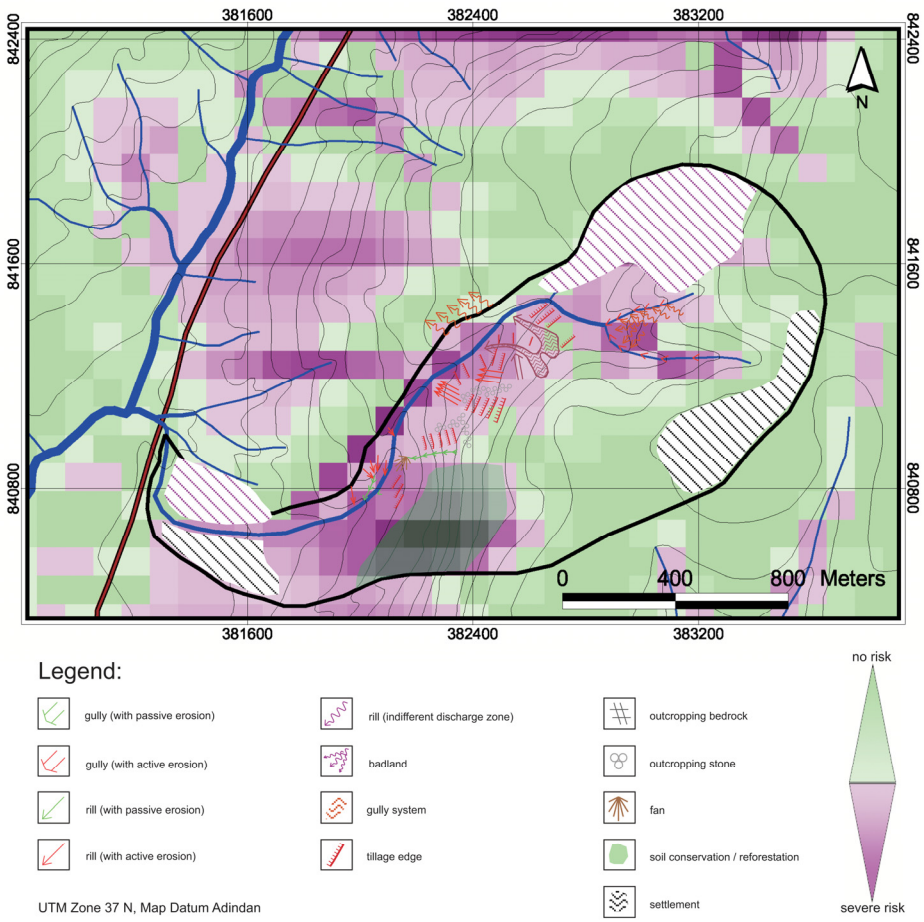

Fig. 98: Damages of the Study Site *'Ana'* superimposed on the Risk Map

9.3.2 Validation

Validation of the model was carried out semi-qualitatively, based on superimpositions of the risk maps on the damage maps that were not utilised for calibration. In addition, the occurrence of gullies mapped randomly outside the study areas was put in correlation to the degree of risk.

The results of the validation show good correlation between damages, the degree of damages and the occurrence of different erosion and soil erosion damages. In fact, highly endangered areas often coincide with the occurrence of badlands, gullies or gully systems, whereas moderate to low risk areas often experience damages from rill and sheet erosion. Figure 99 shows the mapped damages of the study site Sedebo that was not utilised for

calibration on the model. Also here, high erosion and soil erosion risk coincide with mapped gullies and badlands, whereas areas of no risk experience in the field accumulation areas.

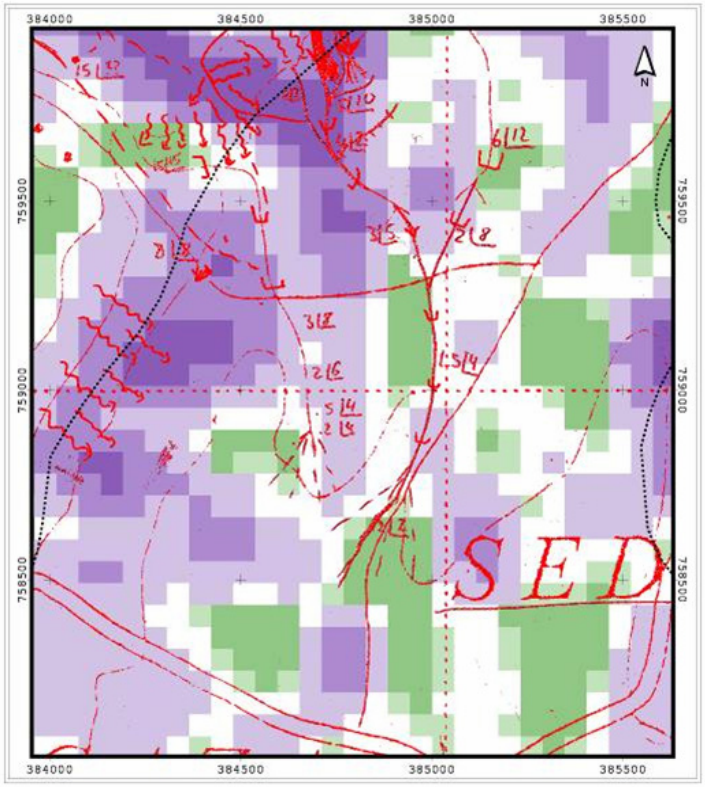

Fig. 99: Damages of the Study Site '*Sedebo*' superimposed on the Risk Map

Similar results are shown in figure 100. The erosion and soil erosion risk classes are plotted against the numbers of gullies that were randomly mapped in the watershed. No gullies were mapped in areas of risk classes smaller than six and the risk class where most gullies have been recorded is the class 13, whereas classes in between show a relatively small number of mapped gullies.

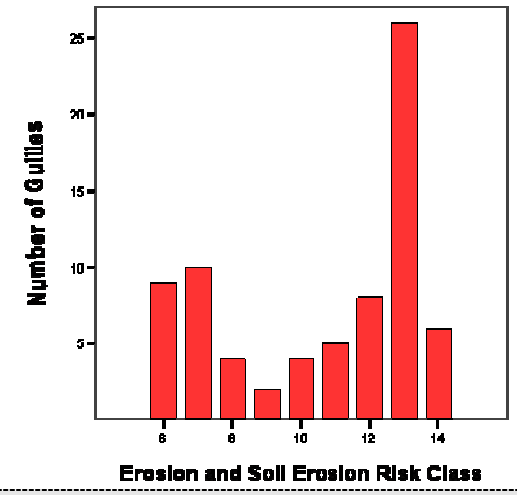

Fig. 100: Erosion and Soil Erosion Risk Classes versus Number of Gullies

9.4 Scenarios

The model DESER allows a high variety of scenarios based on the needs of its users. Two different applications are highlighted in the following section.

Based on the information discussed above, the actual erosion and soil erosion risk was modelled for the entire watershed. The result is exemplarily illustrated for a partial region in figure 101 (left picture). REUSING (2000) designed a method for the estimation of population density and its growth. He assumes six persons living in one *tukul* and an average population growth of 2.23% per year. The number of *tukuls* is known from topographical maps and aerial photographs. Based on these data, the numbers of *tukuls* were recalculated for a 20 years time log and distributed by chance across the watershed. In the model, the numbers of *tukuls* were one indicator to assess actual erosion and soil erosion risk and thus, a scenario was modelled that is based on population growth (fig. 101, right picture). In addition, an increase in soil erodibility was assumed to account for the likely intensification of land use. The result shows a general shift to more risky classes and a significant increase in high to very high risk classes. The scenario approaches were designed during a student's internship of the universities FU Berlin and Siegen in Ethiopia.

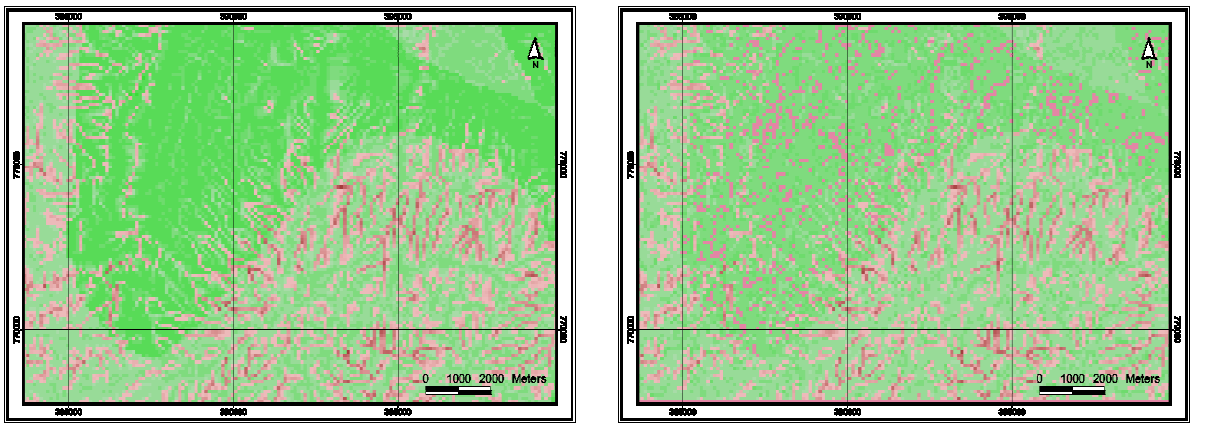

Fig. 101: Actual Erosion and Soil Erosion Risk before (a) and after doubled population (b)

Another application of the model DESER allows reverse conclusions about changes of the land cover class based on population growth and thus, the increase in erosion and soil erosion risk. Figure 102 (left picture) displays the LCCI for the central part of the *Rift Valley*. Grey colour is representing the LCCI class 'six - unconsolidated material' and dark green represents the LCCI class 'one - very green'. In addition, the *tukuls* are displayed as indicator for the population density. On the right picture (fig. 102) the population density doubled, again demonstrated by the numbers of *tukuls*. It is assumed, that irregular settlement

patterns took place where the LCCI class six was absent at the start of the modelling. Erosion and soil erosion risk multiply and consequently erosion damages increase. Vegetation cover is directly affected by the enhanced erosion and soil erosion damages, leading to a shift of the LCCI to lower classes. This scenario was observed in smaller dimensions in the area of the study site '*Dimtu*', where a farmer explained similar experiences (appendix, interview 2).

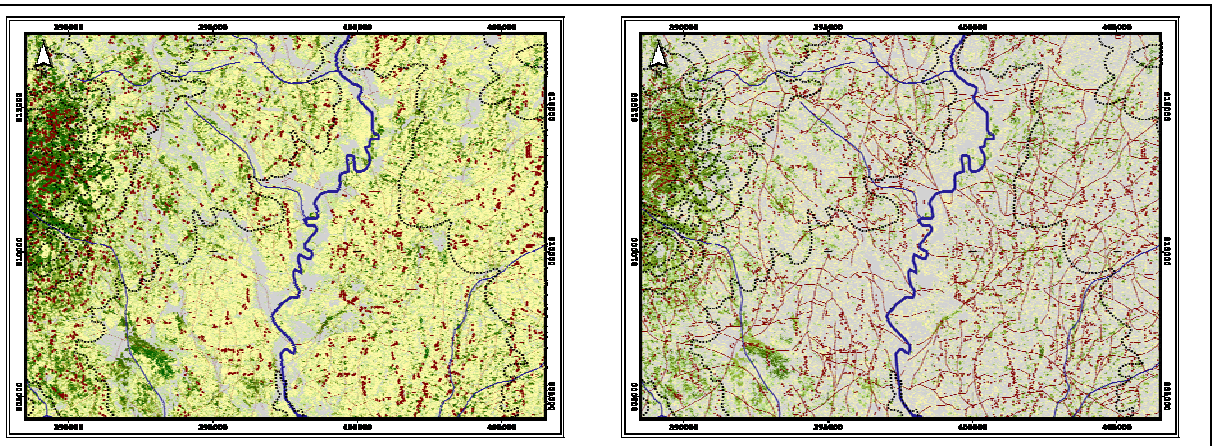

Fig. 102: Vegetation Cover in the Central Part of the *Rift Valley* before (a) and after doubled population (b)

The model DESER was developed for applications of regional planning institutions. One potential approach to address the above illustrated scenario could be the strengthening of regional planning. Figure 103 shows such a potential approach, proposing the concentration of populations in urban areas. The left part illustrates the current situation. To avoid the above scenario, *tukuls* were concentrated in the south-western area representing a town and other *tukuls* were removed. In addition, the number of *tukuls* was doubled. The right side clearly highlights the general shift of the LCCI to lower classes in the mountainous areas and within the town, but major parts of rural areas experience a shift to higher LCCI values.

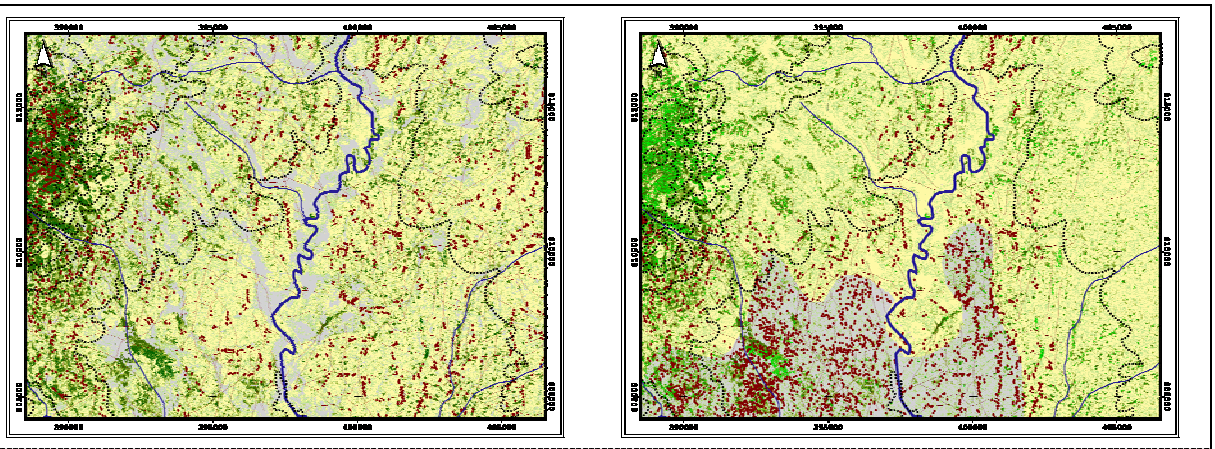

Fig. 103: Vegetation Cover in the Central Part of the Rift Valley before (a) and after Regional Planning Measures (b)

Using the same scenario, the erosion and soil erosion risk is highlighted in figure 104. Instead of widespread endangerment (left picture), the high risk areas are concentrated in the south-west where the virtual town is located, whereas in other regions the actual erosion and soil erosion risk decreases due to lower population density.

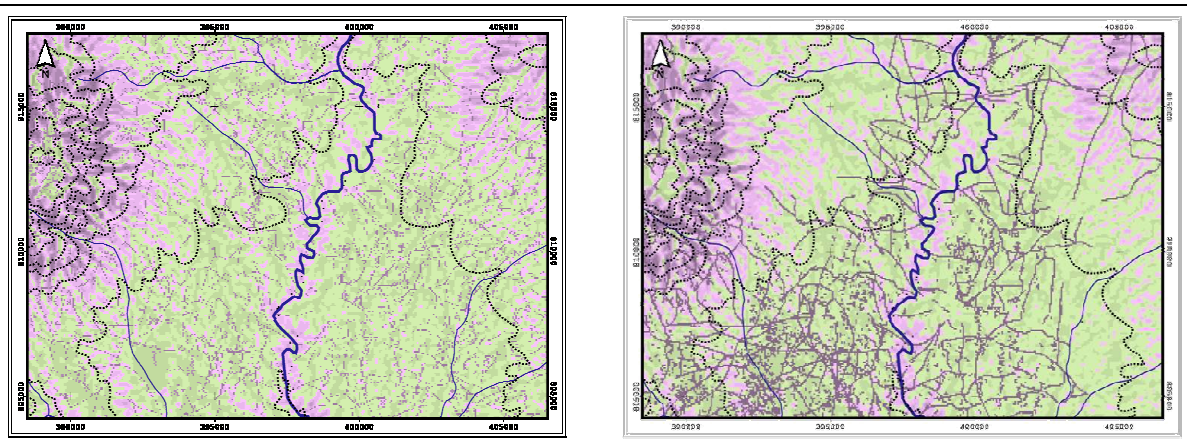

Fig. 104: Increasing actual Erosion and Soil Erosion Risk without a) and with Regional Planning b)

9.5 Limitations

This section discusses temporal, scale, spatial and accuracy limitations of the DESER model.

Temporal limitations are caused by geo-factors that are relevant to erosion and soil erosion. Since damages from the splash effect, inter-rill and rill erosion, and gully erosion were considered for calibrating the model, only time scales during which all the individual processes happen are in theory the minimal temporal limitation. The splash effect is a process of milliseconds, but the development of gullies can take several hours or months. Thus, the minimal timeframe for modelling actual erosion and soil erosion risk could be daily. This also depends on the availability of precipitation total and intensity data. In this research, only monthly average precipitation totals were incorporated into the model and thus, the minimal timeframe for modelling is monthly. The maximal timeframe also depends on the availability of precipitation data. However, when increasing the timeframes for modelling, different geo-factors obtain more relevance, whereas others lose significance. RENSCHLER & HARBOR (2002) illustrate that the assessment of erosion and soil erosion requires a time log of up to one year for the input parameters that were incorporated into this model. Thus, the maximal timeframe for modelling should not exceed one year. This is also limited to the LCCI which can only be determined for a single season.

The scale limitation is not of traditionally known scale problem, since the model is working on grid data sets independent of the amount of grid numbers. Limitations are the size of the grids cells and the computer capacity for modelling. Best performance was reached when using grids sizes of 100 by 100 meters. Base data from SRTM and satellite images were suggested and a compromise was found between the spatial input factors for determining the potential erosion and soil erosion risk and the input data that were incorporated to assess the actual erosion and soil erosion risk. These data are theoretically of higher precision and can also be represented as grid data with grid sizes of 50 by 50 meters. Attempts to model this grid size failed due to the computer capacity of a standard office computer (5,500 km² divided by 10,000 m² [cell size 100 by 100 meters] result in 550,000 cells for each single input parameter; 5,500 km² divided by 2,500 m² [cell size 50 by 50 meters] result in 2.2 mio cells). An attempt of partially modelling the area in higher resolution resulted in higher accuracy, but this accuracy could not be validated with ground data. A more detailed output does not automatically lead to higher accuracy. An additional general limitation for this model is given by the size of the research area: the bigger the research area, the more resources have to be used to calibrate the model, since the variety of landscape characteristics could increase.

The model was developed for semi-arid to semi-humid areas. Various studies throughout the last decades highlight that models cannot be transferred from one area to another without multiple uncertainties, which have to be considered again for each region. Therefore, this model cannot be universally adapted to other regions without some adjustments. However, the amount of input factors is very limited and partially generalised; a transformation to other regions should not lead to unsolvable problems or higher uncertainties. Thus, this model is not limited in its spatial application, as long as it is utilised within the above-mentioned conditions.

The accuracy of the model DESER in relation to other erosion and soil erosion prediction models is imprecise. The model is qualitative and thus, the output is presented as a qualitative classification of erosion and soil erosion risk. Since the aim of this model is to be simple and easy to use by a range of users, such as regional planners, scientific purposes were considered for the development of the model but not for its application. However, the accuracy of modelling is enhanced by the calibration, which is based on ground mapping. Thus, the quality of this model strongly depends on the qualification of users who conduct the field surveys and analyze their results. Geographical knowledge is indispensable to perform good calibration and thus, modelling.